edge (Region 1, or "ring" region); (2) intermediate EPD occurs in the center (Region 2, or "center" region); (3) maximum EPD occurs at the edge (Region 3, or "edge" region). In addition, the EPD in the ring and edge regions is greater along the $< 100 >$ than the $< 110 >$ direction (See figure 4). Figure 5 indicates measured EPD distributions across the full diameter of wafers which typically followed a "W"-shaped profile, and invariably increased from front to tail, indicating that the overall level of stress increased along the crystal, or that the dislocations multiplied after growth, or both. It is important to note that the EPD values at the center and ring regions represent over 75% of the area of the wafer. Therefore, the averaged EPD from these two areas is indicative of the EPD value for the entire wafer. Our experimentally determined radial EPD distributions are consistent with theoretical thermoelastic analyses of Czochralski crystals by Penning (ref. 13) and Jordan et al. (refs. 15, 16).

Through the use of good quality seeds (EPD < 5000 cm^{-2}), seed necking (if EPD > 5000 cm^{-2}), shallow cone shaping ($\sim 30°$), thicker B_2O_3 encapsulant layers, and good diameter controls ($< \pm$ 3mm), we have routinely produced 3-inch undoped LEC GaAs crystals with significantly reduced dislocation densities as shown in table I. Further reductions have been attained at the front of the crystal using a slightly As-rich melt, low ambient ($\sim$ 3 atm) pressures (see table I), or Se-doping ($[Se] \sim 3 \times 10^{18} cm^{-3}$)(see table II). Dislocation densities as low as 6000 cm^{-2} were observed, which is the lowest density reported for 3-inch diameter LEC GaAs wafers. Finally, substantial reduction in dislocation density ($\sim 3.5 \times 10^{4} cm^{-2}$) has also been achieved at the tail of the crystal through a slow pull-free process, as shown in table I. In contrast to the regular fast pull-free process used to terminate the crystal growth process, the pull-rate did not increase in the slow pull-free process in order to significantly reduce the thermal shock during the pull-free process.

No dislocation reduction effect was observed for Si or Zn doping up to 2×10^{18} and $1 \times 10^{19} cm^{-3}$, respectively. In contrast to Bridgman growth (ref. 17), a higher dislocation density was observed in Si-doped LEC GaAs crystals as compared to that of the undoped crystals. The result can be explained by the viscosity reduction in the B_2O_3 encapsulant (i.e. increasing thermal stress) due to the increase of Si content in B_2O_3 (ref. 18).

Our EPD results observed in the present study (see tables I and II) are comparable to commerical 2-inch, undoped D-shaped Bridgman-grown GaAs, as shown in table III. Moreover, the observed values are at least 5 to 10 times lower than commercial 2-inch and 3-inch LEC GaAs crystals (see table III).

Reduction of Twinning

A major problem which has affected the yield of GaAs material suitable for device processing has been the incidence of twin formation. We have found that the melt stoichiometry is an important parameter in controlling the formation of twins in 3-inch-diameter, (100)LEC GaAs crystals. The results of our study show that the incidence of twinning is considerably reduced when undoped or doped crystals are grown from As-rich, near stoichiometric melts. Only 4 or 12 (33%) undoped crystals grown from Ga-rich melts were single. On the other hand, 11 of 13 (85%) undoped crystals and 8 of 9 (90%) doped crystals grown from As-rich melts were single. Furthermore, the incidence of twinning could not be correlated with other growth parameters, such as the wetness of B_2O_3 (for $[H_2O] <$ 500 ppm), the

cone angle, the fluctuation in the diameter of the crystal, or the type of the crucible. The achievement of high single crystal yield (~ 90%) in the LEC GaAs crystals indicates a significant advantage over the conventional Bridgman growth technique, in which the single crystal yield is usually substantially reduced by the crystal sticking to the boat.

Microstructures Observed by TEM

In general, microstructures free of stacking faults, low-angle grain boundaries and dislocation loops, except a few dislocations, can be observed for all undoped LEC GaAs crystals, as well as crystals with Se, Si and Zn doping up to 2×10^{18}, 3×10^{18} and $1 \times 10^{19} cm^{-3}$, respectively. However, as the Se doping increases to greater than $2 \times 10^{18} cm^{-3}$, stacking faults and dislocation loops, as shown in figure 6, can be observed. Our results are consistent with that of high-quality Bridgman-grown materials.

Background Impurities

The averaged concentrations of background shallow-donor (Si, S, Se and Te) and metal (Mg, Cr, Mn, Fe and B) impurities in the 3-inch-diameter LEC GaAs grown from both quartz and PBN crucibles as determined by SIMS measurements are shown in table IV. With the exception of Si and B the impurity concentration levels are exceedingly low. Many measurements are either at or below the typical background sensitivity of SIMS technique, suggesting that LEC material in some cases is purer element-by-element than the standard used to check the SIMS background sensitivity. The concentration of both Si and B range from 1×10^{14} to $3 \times 10^{16} cm^{-3}$, and from 6×10^{14} to $2 \times 10^{18} cm^{-3}$, respectively. B is the isoelectronic impurity in GaAs, no indication of the electrical activity of B in LEC GaAs has been observed. C as determined by LVM measurements is present at levels varying from about less than $\sim 1 \times 10^{15} cm^{-3}$ (detection limit) to $1.3 \times 10^{16} cm^{-3}$. Therefore, C is expected to be a dominant acceptor in LEC material.

We have found that the variability in Si and B levels is dependent on variations in the H_2O content of the B_2O_3 (ref. 19). H_2O in the encapsulant reduces the transport of Si through the B_2O_3 from the quartz crucible to the melt. In addition, the presence of H_2O reduces the pick-up by the melt of B from the B_2O_3. Si-doped, n-type LEC GaAs with an electron density less than $5 \times 10^{16} cm^{-3}$ can, therefore, only be grown from quartz crucibles using "dry" B_2O_3 ($[H_2O] < 500$ ppm).

Our analysis of the background metal impurities, such as Fe, Cr, and Mn, shows virtually no difference between LEC and Bridgman material, as indicated in table IV. The background concentration of the residual donor S is also comparable. Although the Si concentration varies in LEC material grown from quartz crucibles, Si contamination is virtually eliminated by growing from PBN crucibles. As a result, the background Si concentration in LEC GaAs is typically more than one order of magnitude lower than in Bridgman material. Our highest purity material had a concentration of total donors and acceptors ($N_D + N_A$) of about $4 \times 10^{15} cm^{-3}$, but the typical purity is about $1\text{-}2 \times 10^{16} cm^{-3}$.

Mobility

The dependence of the electron mobility on the free carrier concentration of our material is shown in figure 7. The Se-doped LEC samples have a mobility of approximately 4000 and 2500 $cm^2/Vsec$ corresponding to electron densities of 1×10^{17} and $1 \times 10^{18} cm^{-3}$, respectively. A slightly lower mobility is observed for the Si-doped samples indicating higher compensation. In general, the mobility curves show a peak for an electron density of $\sim 10^{17} cm^{-3}$. The reduced mobilities at lower electron concentrations are probably due to compensation controlled by background impurities or native defects. Our mobility results are consistent with statistical analysis of hundreds of crystals grown by conventional bulk-grown methods reported recently by Mullin et al. (ref. 20). In addition, a comparison of our results to the theoretical mobility-electron concentration relationship for GaAs, indicates that our material is characterized by low compensation ratios (0.3 to 0.4) consistent with the statistical behavior of other bulk GaAs materials.

Good mobility was also observed for the p-type LEC GaAs, as shown in figure 8. Hole mobilities as high as 330 $cm^2/Vsec$ (for hole concentration $\sim 1 \times 10^{16} cm^{-3}$) were observed for the LEC material grown from undoped Ga-rich melt using a PBN crucible. Mobilities as high as 210 $cm^2/Vsec$ were observed for Zn-doped material with $\sim 4 \times 10^{17} cm^{-3}$ hole concentration. Elliott et al. (ref. 21) have explained the p-type conduction of the undoped LEC GaAs in terms of the 77 meV acceptor (ref. 22). The origin of this acceptor is probably the Ga_{As} antisite defect. Our mobility results for the p-type LEC GaAs are also comparable to the comemrcially-available, high-purity, small-diameter Bridgman-grown GaAs, as shown in figure 8.

Minority Carrier Diffusion Length

Good hole diffusion lengths (as high as 1.3 μm) have been observed for n-type (Se- or Si-doped), 3-inch-diameter LEC GaAs crystals, as shown in figure 9. The measured values are comparable to those of n-type bulk GaAs grown by conventional methods reported by Sekela et al. (ref. 12). The electron diffusion length has only been determined for one p-type undoped LEC GaAs crystal grown from Ga-rich melt in a PBN crucible (table V). A diffusion length as high as 5.3 μm is observed in the material. This value is close to the 8 μm electron diffusion length reported for both p-type high-purity MOCVD and LPE layers (refs. 10, 11 and 23).

No correlation was observed between the dislocation density and diffusion length for either n- or p-type LEC GaAs. A similar observation has been reported by Sekela et al. (ref. 12) for n-type bulk GaAs. Finally, it is of interest to note that the hole diffusion length as well as the hole concentration across the full-diameter wafer decrease towards the edge, as shown in table V. Since a constant hole mobility was observed across the wafer and no correlation between the diffusion length and dislocation density was detected, the decrease of the diffusion length may be attributed to an increase of an unknown donor concentration toward the edge of the wafer. Further work is still needed in this area.

CONCLUSION

We have shown that large-diameter, n- and p-type LEC GaAs can be grown with a low-dislocation-density, high purity, long minority carrier diffusion lengths, and high mobility. A high single crystal yield (~ 90%) and clean microstructures have also been achieved in these materials. The properties are comparable to small-diameter GaAs crystals grown by conventional bulk growth techniques. Our results showing low dislocation densities and long diffusion lengths indicate that the dislocation density will not be a limiting factor for the application of 3-inch-diameter LEC GaAs crystals to minority carrier devices, such as solar cells. The low background impurities, consistent with high mobility and long diffusion length, also ensure the use of these materials as both passive and active substrate materials in these devices. We, therefore, conclude that for minority carrier devices requiring high-quality and large-area substrates, the 3-inch-diameter LEC GaAs crystals are indeed an excellent material for such applications.

REFERENCES

1. AuCoin, T.R.; Ross, R.L.; Wade, M.J.; and Savage, R.O.: Liquid Encapsulated Compounding and Czochralski Growth of Semi-Insulating Gallium Arsenide, Solid State Technology, vol. 22, no. 1, 1979, pp. 59-62.

2. Mullin, J.B.; Heritage, R.J.; Holliday, C.H.; and Straugham, B.W.: Liquid Encapsulation Crystal PUlling at High Pressure, J. Crystal Growth, vol. 3-4, 1968, pp. 281-285.

3. Fairman, R.D.; Chen, R.T.; Oliver, J.R.; and Ch'en, D.R.: Growth of High-Purity Semi-Insulating Bulk GaAs for Integrated-Circuit Applications, IEEE Transactions on Electron Devices, vol. ED-28, no. 2, 1981, pp. 135-140.

4. Holmes, D.E.; Chen, R.T.; Elliott, K.R.; and Kirkpatrick, C.G.: Stoichiometry-Controlled Compensation in Liquid Encapsulated Czochralski GaAs, Appl. Phys. Lett., vol. 40, no. 1, 1982, pp. 46-48.

5. Holmes, D.E.; Elliott, K.R.; Chen, R.T.; and Kirkpatrick, C.G.; Stoichiometry-Related Centers in LEC GaAs, 2nd Conference on Semi-Insulating III-V Materials, Evian, France, April 19-21, 1982.

6. Thomas, R.N.; Hobgood, H.M.; Eldridge, G.W.; Barrett, D.L.; and Braggins, T.T.: Growth and Characterization of Large Diameter Undoped Semi-Insulating GaAs For Direct Ion Implanted FET Technology, Solid-State Electronics, vol. 24, 1981, pp. 387-399.

7. Dash, W.D.: Growth of Silicon Crystals Free of Dislocations, J. Appl. Phys., vol. 28, no. 8, 1957, p. 882.

8. Brozel, M.R.; Clegg, J.B.; and Newman, R.C.: Carbon, Oxygen and Silicon Impurities in Gallium Arsenide, J. Phys. D, Appl. Phys., vol. 11, 1978, pp. 1331-1339.

9. Hackett, W.H., Jr.: Electron-Beam Excited Minority-Carrier Diffusion Profiles in Semiconductors, J. Appl. Phys., vol. 43, no. 4, 1972, pp. 1649-1654.

10. Shen, C.C.; Pande, K.P.; and Pearson, G.L.: Electron Diffusion Lengths in Liquid-Phase Epitaxial p-GaAs:Ge Layers Determined by Electron-Beam-Induced Current Method, J. Appl. Phys. vol. 53, no. 2, 1982, pp. 1236-1237.

11. Wight, D.R.; Oliver, P.E.; Prentice, T.; and Steward, V.W.: Diffusion Lengths In p-type MOCVD GaAs, J. Crystal Growth, vol. 55, 1981, pp. 183-191.

12. Sekela, A.M.; Feucht, D.L.; and Milnes, A.G.: Diffusion Length Studies in n Gallium Arsenide, Inst. Phys. Conf. Ser. No. 24, 1975, pp. 245-253. (The Fifth International Symposium on Gallium Arsenide and Related Compounds, Deauville, France, 24-26 September 1974).

13. Penning, P.O., Philips Research Reports, vol. 13, 1958, p. 79.

14. Mil'vidskii, M.G.; and Bochkarev, E.P.: Creation of Defects During the Growth of Semiconductor Single Crystals and Films, J. Crystal Growth, vol. 44, 1978, pp. 61-74.

15. Jordan, A.S.; Caruso, R.; and Von Neida, A.R.: A Thermoelastic Analysis of Dislocation Generation in Pulled GaAs Crystals, The Bell System Technical Journal, vol. 59, no. 4, 1980, pp. 593-637.

16. Jordan, A.S.: An Evaluation of the Thermal and Elastic Constants Affecting GaAs Crystal Growth, J. Crystal Growth, vol. 49, 1980, pp. 631-642.

17. Suzuki, T.; Akai, S.I.; Kohe, K.; Hishida, Y.; Fujita, K.; and Kito, N.: Development of Large Size "Dislocation-Free" GaAs Single Crystal, Sumitomo Electric Technical Review, no. 18, December 1978, pp. 105-111.

18. Rasa Co. Japan, Private communication.

19. Oliver, J.R.; Fairman, R.D.; Chen, R.T.; and Yu, P.W.:Undoped Semi-Insulating LEC GaAs: A Model and A Mechanism, Elec. Letts., vol. 17, no. 22, 1981, pp. 839-841.

20. Mullin, J.B.; Royle, A.; and Benn, S.: A Study on the Relationship Between Growth Technique and Dopants on the Electrical Properties of GaAs With Special Reference to LEC Growth, J. Crystal Growth, vol. 50, 1980, pp. 625-637.

21. Elliott, K.R.; Holmes, D.E.; Chen, R.T.; and Kirkpatrick, C.G.: Infrared Absorption of the 78 meV Acceptor in GaAs, Appl. Phys. Lett., May, 1982.

22. Yu, P.W.; Holmes, D.E.; and Chen, R.T.: Photoluminescence Study in LEC GaAs, Int. Symp. on GaAs and Related Compounds, Oiso, Japan, September 20-23, 1981.

23. Casey, H.C.; Miller, B.I.; and Pinkas, E.: Variation of Minority-Carrier Diffusion Length with Carrier Concentration in GaAs Liquid-Phase Epitaxial Layers, J. Appl. Phys., vol. 44, no. 3, 1973, pp. 1281-1287.

TABLE I. DISLOCATION DENSITY REDUCTION IN UNDOPED 3-INCH LEC GaAs

Front (cm^{-2})	Tail (cm^{-2})
1) 12×10^3 ($6 \times 10^{3*}$)	9.0×10^4 ($3.3 \times 10^{4+}$)
2) 1.8×10^4 ($1.3 \times 10^{4*}$)	1.0×10^5 ($3.5 \times 10^{4+}$)
3) 2.0×10^5 ($9 \times 10^{4*}$)	2.2×10^5 ($1.1 \times 10^{5+}$)

*Grown by low ambient pressure (~ 3 atm)
+Grown by slow pull-free process

TABLE II. DISLOCATION DENSITY REDUCTION IN DOPED 3-INCH LEC GaAs*

Front (cm^{-2})	Tail (cm^{-2})
1) 6×10^3	1) 6.1×10^4
2) 1.1×10^4	2) 1.2×10^5
3) 1.7×10^5	3) 1.7×10^5

*Se-doping ($n_e \sim 2 \times 10^{18} cm^{-3}$)

TABLE III. DISLOCATION DENSITY FOR COMMERICALLY AVAILABLE 2-OR 3-INCH BRIDGMAN AND LEC GaAs CRYSTALS

	E.P.D. (cm^{-2})
2 INCH - Bridgman (D-shaped)	$\sim 2 \sim 3 \times 10^4$
LEC	$\geqslant 4 \times 10^4$
3 INCH - LEC	$> 4 \times 10^4$ (Front) $> 3 \times 10^5$ (Tail)

TABLE IV. BACKGROUND IMPURITY ANALYSIS OF LEC GaAs

GROWTH TECHNIQUE	CRUCIBLE	S	Se	Te	Mg	Cr	Mn	Fe	C*	Si	B
LEC[a]	QUARTZ	1.3e15	<1e14	<1e14	<5e14	<5e14	<1e15	<3e15	~3e15 (ND-9e15)	5e14-3e16	4e14-2e17
LEC[b]	PBN	1.1e15	<5e14	<5e13	2e14	<5e14	<1e15	<3e15	2-13e15	<1e15	4e14-2e17
BRIDGMAN[c]	QUARTZ	3e15	3e14	4e13	5e14	<5e14	5e14	5e15	ND	2e16	<2e14

[a] 7 CRYSTALS ANALYZED AND AVERAGED.

[b] 12 CRYSTALS ANALYZED AND AVARAGED.

[c] 4 CRYSTALS ANALYZED AND AVERAGED.

*CARBON DETERMINED BY LVM.

TABLE V. ELECTRON DIFFUSION LENGTH IN P-TYPE LEC GaAs

WAFER NO.	CRUCIBLE	DOPANT	SAMPLE LOCATION	FREE HOLE CONCENTRATION (cm^{-3})	DIFFUSION* LENGTH (μm)	MOBILITY ($cm^2/Vsec$)
R20-F	PBN	NONE	CENTER	1.33×10^{16}	5.3	315
		(Ga-RICH MELT)	RING	1.10×10^{16}	4.1	315
			NEAR EDGE	1.05×10^{16}	2.3	316

*ELECTRON DIFFUSION LENGTH ~8 μm REPORTED FOR BOTH p-TYPE MOCVD AND LPE LAYERS.

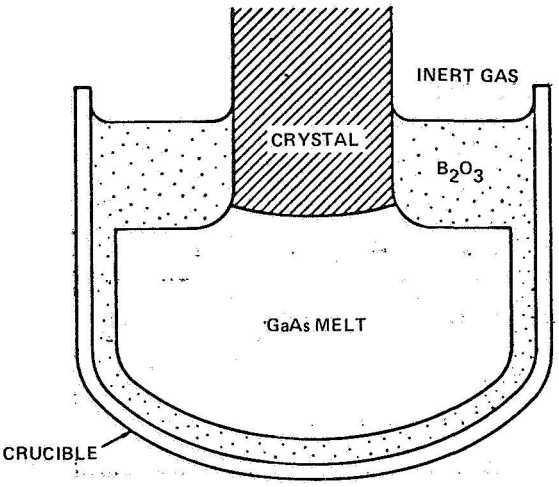

Figure 1. Configuration for LEC Growth System.

Figure 2. A 3.6 Kg, 3-inch Diameter, (100) LEC GaAs Crystal with Diameter Variation Less Than ± 2mm.

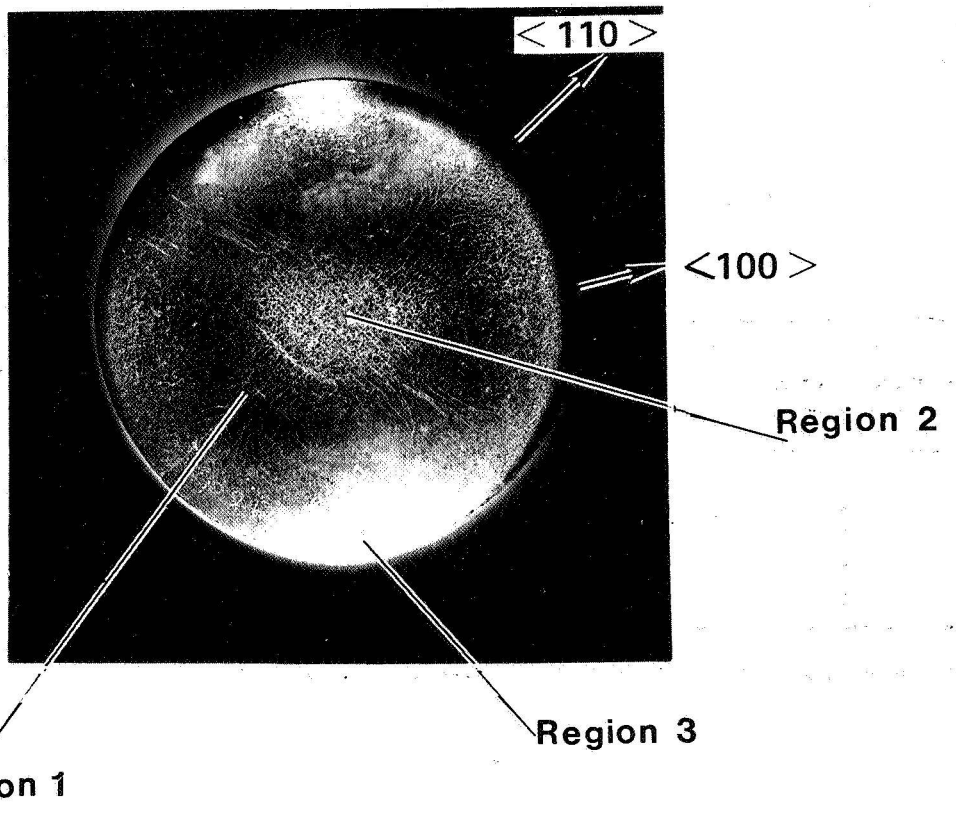

Figure 3. Radial Dislocation Density Map for 3-inch GaAs LEC wafers.

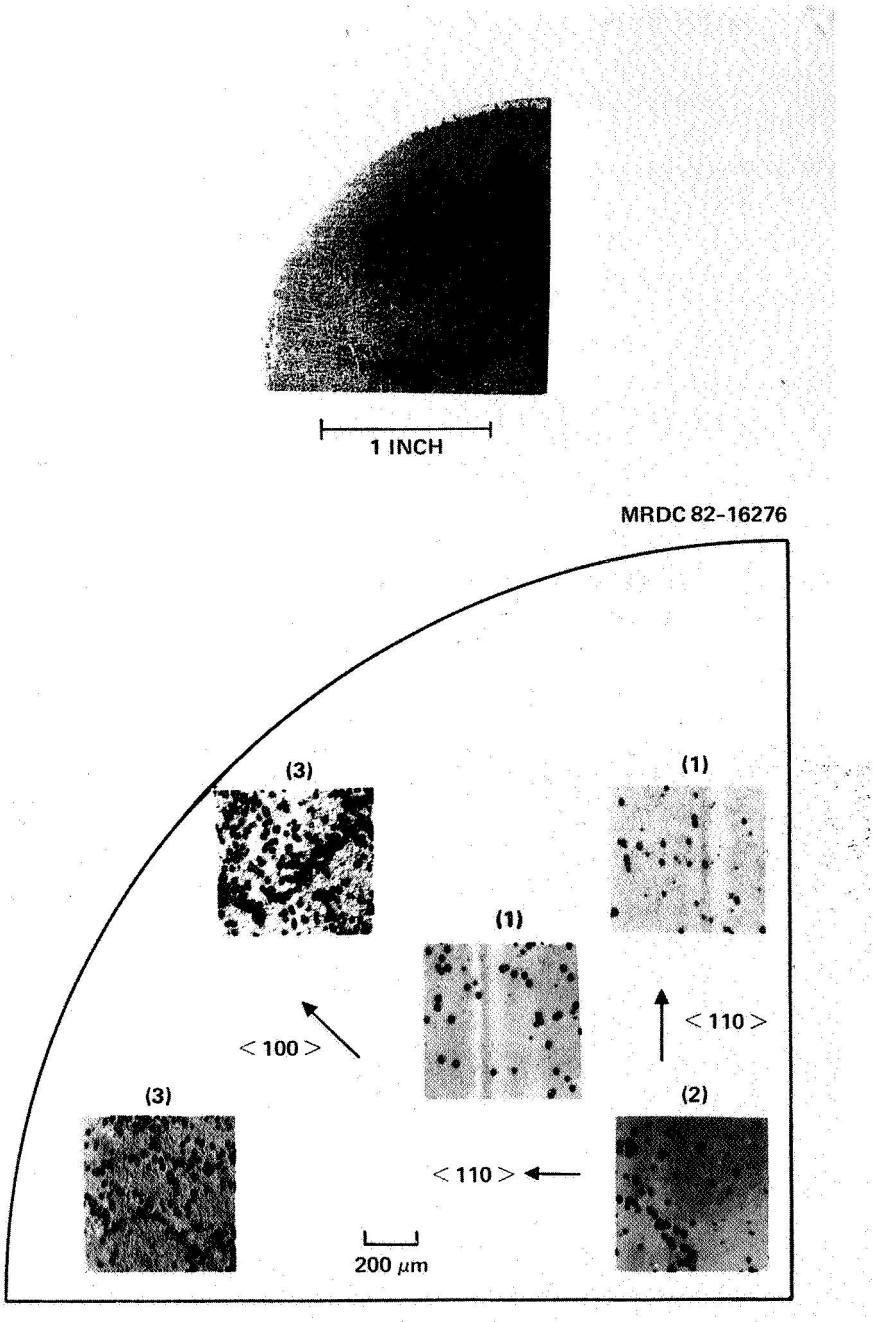

Figure 4. Etch Pit Density Map for a (100) LEC GaAs Wafer.

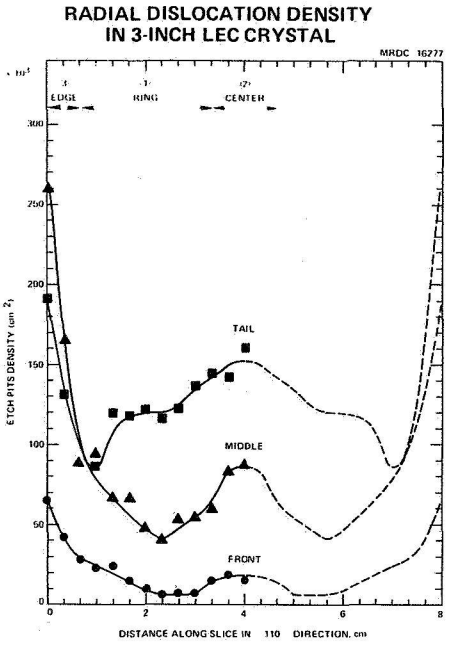

Figure 5. Radial and Longitudinal Dislocation Density for Large-diameter LEC GaAs Crystal.

Figure 6. B.F. Micrograph for a Se-doped LEC GaAs sample with [Se] ~ 7 x 10^{18}cm^{-3}.

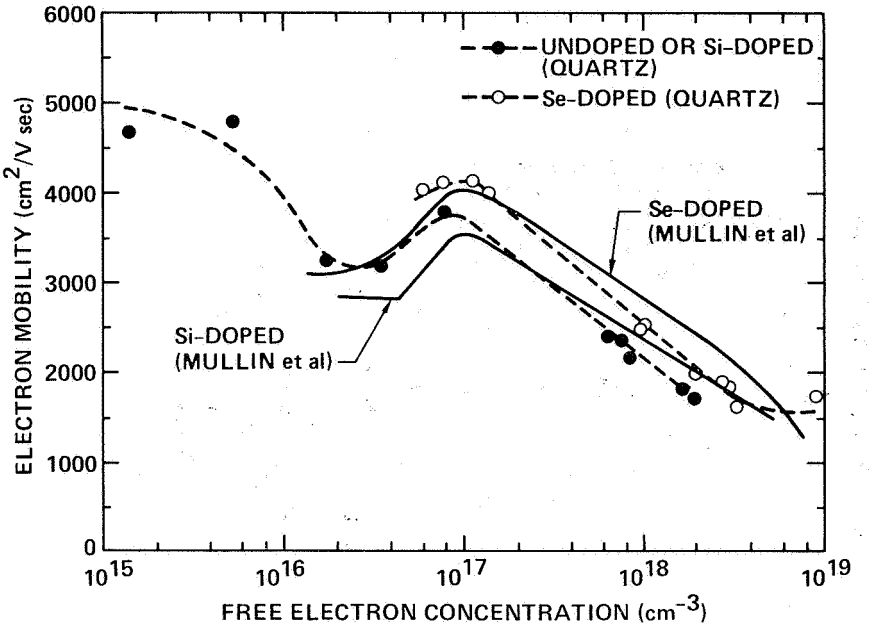

Figure 7. Mobility vs. Free Electron Concentration for n-type LEC GaAs.

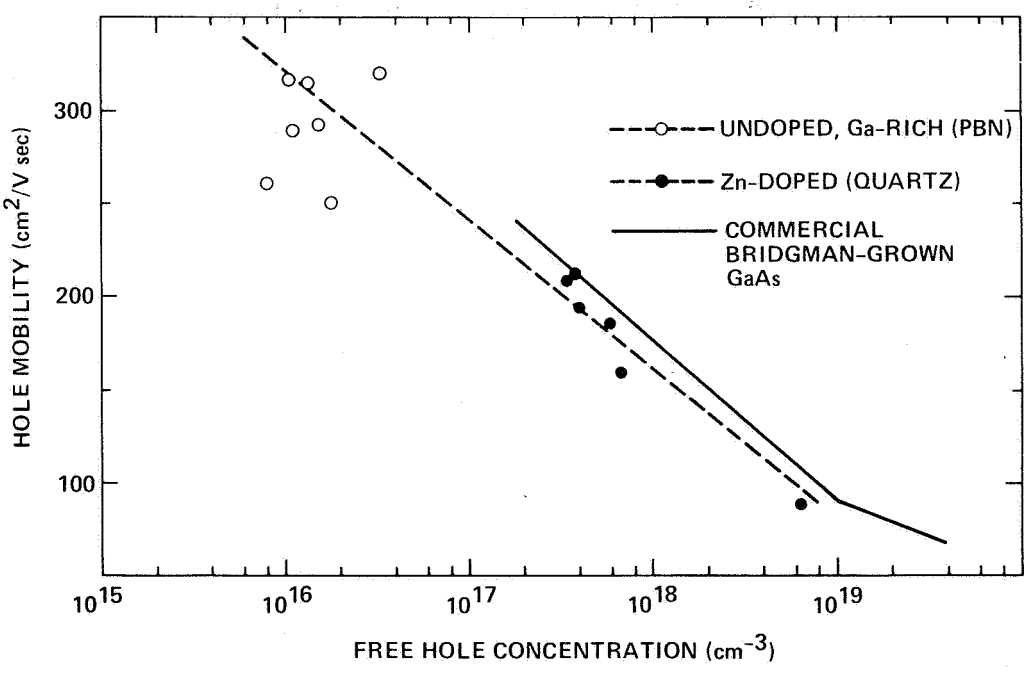

Figure 8. Mobility vs. Free Hole Concentration for p-type LEC GaAs.

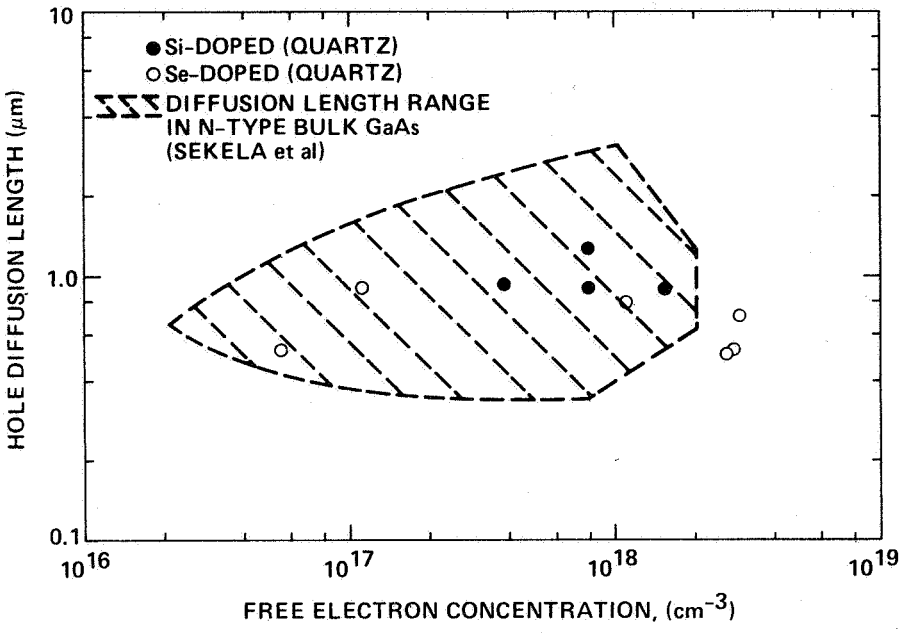

Figure 9. Hole Diffusion Length vs. Free Electron Concentration for n-type LEC GaAs.